Seasonally-decomposed Sentinel-1 backscatter time-series are useful indicators of peatland wildfire vulnerability

Authors: Millard, Koreen[a]*, Darling, Samantha[a], Pelletier, Nicolas[a], Schultz, Samantha[a]

a - Department of Geography and Environmental Studies, Carleton University, 1125 Colonel By Drive, Ottawa, Ontario, Canada, K1S5B6

*corresponding author: koreen_millard@carleton.ca

** This is a preprint submitted to EarthArXiv. It has been peer-reviewed and accepted for publication in the journal Remote Sensing of the Environment (https://doi.org/10.1016/j.rse.2022.113329)**

Abstract

Peatlands throughout the boreal forest are expected to experience changes in precipitation, evapotranspiration and temperature due to climate change. Correspondingly, changes in hydrologic regimes could lead to increased drought and occurrence of wildfire. Fire management agencies require information about near-real time wildfire vulnerability in boreal peatlands. Remote sensing tools (*e.g.*, NDVI, NDII) to monitor changing wildfire vulnerability focus on monitoring changes in vascular vegetation and are not necessarily applicable to moss-dominated peatlands. We use time series analysis of Sentinel-1 SAR backscatter data to compare the trends in peatlands that have burned to unburned peatlands and show that the Theil-Sen slopes of seasonally decomposed SAR backscatter reflects prolonged drought conditions that can lead to burning. Seasonally decomposed Sentinel-2 NDVI and NDII were also tested but no statistical differences were found between burned and unburned peatlands. Overall, we found that 6 months prior to a wildfire the slope of seasonally decomposed Sentinel-1 VV SAR backscatter was significantly different in burned and unburned peatlands, and can be used to spatially identify fire vulnerability and identify fire-prone areas.

1. Introduction

Canada's boreal forest is forecast to experience changes in precipitation, evaporation, and temperature due to climate change (Price et al., 2013), which will lead to changes in hydrological regimes, drought frequency and intensity, and almost certainly, wildfire activity (Coogan et al., 2019). Peatlands are a common landscape throughout the boreal forest (Wieder and Vitt, 2006), where wildfire acts as the dominant disturbance (Thompson et al., 2019). Although peatlands have historically been considered saturated ecosystems that largely avoid fire impact, reduced precipitation and increased temperatures are expected to lower water tables and enhance moss

drying. Both natural and anthropogenic disturbances can lead to changes in peatland hydrology, which affect hydrologic self-regulation, leading to drying and subsequently the vulnerability to more frequent or severe burning (Turetsky et al., 2015). Given an ignition source, sufficiently dry *Sphagnum* and feather mosses can burn and smolder over an extended period of time (Benscoter et al., 2011). The widespread drying of peatlands during drought can trigger a network effect, connecting previously isolated, highly flammable upland forests, which allows for larger wildfires than otherwise possible under normal wetness conditions (Thompson et al., 2019). Instances of multi-year drought have also been documented in boreal peatlands, and in particular, in sites that experienced large wildfires after sustained drought (Elmes et al, 2018).

Smoldering peatland fires are common, yet difficult to detect as they occur in the surface mosses (in Sphagnum or other mosses) or the peatland subsurface (in dry, partially decomposed peat), rather than in canopy or underbrush vegetation. Such fires can burn overwinter, resulting in spring fire activity in boreal forests (Elmes et al, 2018). Smoldering fires result in extended durations of heat transfer, which enable a deeper burn and the loss of carbon stored in deep peat. Deep peat layers represent the oldest soil carbon reserves, which have not been part of the active carbon cycle for hundreds to thousands of years (Turetsky et al., 2015). The release of carbon stored in deep peat (*i.e.*, through combustion) could represent a significant contribution to carbon emissions (Tarnocai, 2009). Smoldering peat fires also result in diminished air quality, regional haze and reduced light levels, which can suppress plant CO_2 uptake, and have effects on human health (Turetsky *et al.*, 2015), (Hu *et al.*, 2018).

National forest fire danger rating systems are used by wildfire management agencies to monitor surface conditions throughout forests globally (Tian *et al.,* 2005). However, peatland fire vulnerability is not explicitly captured in many of these. For example, the Canadian Forest Fire Danger Rating System model (CFFDRS), the system on which many other national fire danger rating systems are based (Tian *et al.,* 2005), currently uses weather-only based metrics (*e.g.,* Fire Weather Index; Tian *et al.,* 2005; Waddington *et al.,* 2011). To accurately apply these metrics across Canada's boreal peatlands would require a dense monitoring network of meteorological conditions (*i.e.*, precipitation, temperature) that is currently not available across most of northern Canada. The installation of such a system throughout the vast boreal forest is not practical nor economically feasible, making earth observation sensors an attractive alternative for monitoring these regions remotely.

Most fire susceptibility and vulnerability modeling has used spatial data, including interpolated weather and climate information (Ghorbanzadeh *et al.,* 2019; Mhawej *et al.,* 2016; Parisien *et al.,* 2012; Valdez *et al.,* 2017), distance to infrastructure (Valdez *et al.,* 2017; Zhang *et al.,* 2016), topography (Ghorbanzadeh *et al.,* 2019; Leuenberger *et al.,* 2018; Parisien *et al.,* 2012; Valdez *et al.,* 2017), fuel type (Michael *et al.,* 2021a), vegetation moisture (Bisquert *et al.,* 2014) and land cover or forest information (Leuenberger *et al.,* 2018; Mhawej *et al.,* 2016; Michael *et al.,* 2021b; Valdez *et al.,* 2017), non-temporal information about vegetation conditions and density (Gray *et al.,* 2018; Valdez *et al.,* 2017). Sometimes spatial data and indices from earth observation sensors are used, such as Normalized Difference Vegetation Index (NDVI) (Bisquert *et al.,* 2014; Hernandez-Leal *et al.,* 2006; Leuenberger *et al.,* 2018; Mhawej *et al.,* 2016; Michael *et al.,* 2021b) or Normalized Difference Moisture Index (NDMI) (Akther and

Hassan, 2011), which are both derived from passive multispectral imagery. Distance to infrastructure is used as a proxy for human causes to wildfire. While some peatland fires are ignited by human activity, many are also caused by lightning strikes, the locations of which are impossible to predict and difficult to monitor. Topographic information does not change (rapidly) temporally so static Digital Elevation Models are appropriate and moderate spatial resolution data is often used (*e.g.,* Shuttle Radar Topography Mission, 30 m spatial resolution). Regional topographic conditions in peatlands generally do not vary greatly (*i.e.,* peatlands are flat and regionally occur at similar elevations) and their important topographic characteristics important to wildfire vulnerability modelling (*e.g.* hummocks and hollows) are not captured by moderate resolution data. Commonly, NDVI and other vegetation indices are used to relate spatial variability in greeness to vegetation chlorophyll content and vegetation health (Lees, 2021) and as contribution to fire fuels (Bisquert *et al.,* 2014), yet few studies have incorporated the temporal or phenologic components of vegetation change in models to predict vulnerability to burning. Exceptions include Michael *et al.,*(2021b), where NDVI was used to derive trends in woody vegetation and Chéret and Denux (2011), where temporal metrics of NDVI were derived for land cover types, which explained spring season greenness and senescence. In related work, Bajocco *et al.,*(2015) used NDVI time series to estimate spatially and temporally variable fuel changes in forests, which could be used as inputs to fire vulnerability models.

Although most literature documents the use of multi-spectral imagery in estimating parameters relevant to calculating fuel moisture and fire danger, SAR has been investigated as a way of mapping both wildfire fuel characteristics (vegetation structure, vegetation moisture/water content and soil moisture) and in fire danger ratings as well. In the past, several authors have

used the ERS-1 satellite (C-band SAR), with most focusing on burned forests due to the improved ability of the sensor to sense both the canopy and ground due to lower vegetation density. Bourgeau-Chavez et al., (1999), Leblon et al., (2002), Bourgeau-Chavez et al., (2007), and Abbott et al., (2007) assessed relationships between several fire weather variables and C-band SAR, generally finding good agreement in boreal and pine forests. Rao et al., (2020) used a combination of optical and Sentinel-1 C-band SAR data to estimate live fuel moisture content across the continental US. They note that multispectral information is representative of plant water content in the top of the canopy whereas SAR may be able to provide information about inner-canopy biomass and vegetation water content. They found that the ratio of microwave backscatter to optical reflectance is similar in nature to the relationship used to estimate live moisture fuel content (fresh mass - dry mass/dry mass). Using deep learning models and Sentinel-1 to predict live fuel moisture in a variety of forested areas across the continental US, Rao et al., (2020) found decreased model performance when SAR was not included (i.e. multispectral imagery used alone).

Several studies have also looked at longer wavelength SAR, or multi frequency SAR in relation to variables relevant to wildfire vulnerability and fuel mapping. Saatchi et al., (2007) used multi-frequency SAR (P-band and L-band) to develop semi-empirical models of variables relevant to stand characteristics and fuel moisture, indicating that L band produced better results in shrub and low density vegetation areas. (Tanase et al., 2014) used L-band Soil Moisture Active Passive (SMAP) and polarimetric airborne SAR data to estimate live fuel moisture and equivalent water thickness in semi-arid Australian forests. Subsequently, Tanase et al., (2015) assessed the relationship between fire severity and SAR at both P-band and L-band in Australian

forests, finding that in low biomass forests, SAR and optical imagery provided comparable results, but general optical data provided a better estimation of (post-fire) severity. Widodo et al., (2018) used a Yamaguchi Decomposition detect tropical peatlands areas from fully-polarimetric L-band ALOS-2 data, and then related InSAR displacement to changes in ground water, concluding that if ground water was less than 40 cm from the surface, the peatlands were potentially combustible. (Kong et al., 2014) assessed the differences between wet and dry images, using Radarsat-2, as a way to indicate changes in fuel moisture in the South African savannah. With the exception of Widodo et al., (2018) which was carried out in a tropical peatland, all studies using SAR were carried out in non-wetland forests. And, with the exception of Rao et al (2020) whose analysis was carried out across the continental US at specific dates, studies were generally carried out at single sites and/or at single time steps or time comparisons. No studies were found using time series of SAR data for fire fuel mapping or fire danger rating.

Whereas most studies aiming to predict wildfire vulnerability use time series analysis, those that include remote sensing data generally use multispectral imagery, focusing on change in vascular vegetation. In peatlands, however, vascular vegetation conditions may not be the most important indicator of wildfire vulnerability. Vascular vegetation is often sparse and peatland fires often occur at the surface in the top layer of mosses, which means surface moisture conditions, water table depths and water table variability play a more important role in regulating their drought status (Waddington *et al.*, 2015; Whitman *et al.*, 2018). While there are indicators of surface wetness that can be derived from multispectral imagery (Arroyo-Mora *et al.*, 2018; Artz *et al.*, 2019; Lastovicka *et al.*, 2020; Meingast *et al.*, 2014), Synthetic Aperture Radar (SAR) data is sensitive to surface wetness conditions (Ulaby, 1974), vegetation structure (Ulaby *et al.*, 1982),

and vegetation water content (Attema and Ulaby, 1978), as well as surface roughness (Mattia *et al.,* 1997). When all other conditions are held the same, as soil moisture decreases SAR backscatter decreases (Ulaby, 1974). However, due to the confounding effects of variability in vegetation and surface roughness, modeling soil moisture in peatlands directly from SAR is not always straightforward (Millard *et al.,* 2018; Millard and Richardson, 2018).

The wide range of spatially and temporally variable "normal" conditions between and within types of peatlands may limit the applicability of static SAR backscatter to an improved understanding of peatland vulnerability to wildfire.

Instead, we hypothesized that a time series of SAR backscatter information may indicate when backscatter has declined over long periods of time (*i.e.,* one growing season, or more), thereby indicating drought. Due to the side-looking nature of SAR and orbits of operational SAR satellites, SAR data are often acquired at several different incidence angles for the same location causing variations in the response of SAR backscatter to soil and vegetation conditions. Based on the requirement for multi-season time series to capture deviations from normal conditions, and the requirement of consistent incident angles at any given site, a sensor that collects data in a consistent configuration is required. One sensor that adheres to these constraints is Sentinel-1, which is a C-Band SAR constellation with 6 or 12 day repeated collection for most of the world (Geudtner *et al.,* 2014). Based on preliminary investigations with time series of Sentinel-1 data, we noted noise in the data (*e.g.,* from speckle) but also a strong cyclic trend, which aligns with seasonality (e.g. using the Tomahawk AB, 2021 fire as an example, Figure 1). Therefore, a statistical technique that can separate the true trend from noise and seasonality is required to

detect the multi-year trend in backscatter. One such technique is *Classical Seasonal Decomposition by Moving Averages* (*R: Classical Seasonal Decomposition by Moving Averages*, 2022), which has been applied by Papacharalampous *et al.*,(2018) and Damrongkulkamjorn and Churueang (2005) for weather and energy consumption forecasting applications, respectively. As NDVI (derived from multispectral data) is used so widely in wildfire vulnerability models, we also applied this decomposition technique to NDVI data calculated from Sentinel-2 imagery (e.g. using the Tomahawk AB, 2021 fire as an example, Figure 2). Since the Normalized Difference Infrared Index (NDII) has been shown to be related to surface conditions in peatlands (Neta *et al.*, 2011), we also tested this technique using time series of NDII (e.g. using the Tomahawk AB, 2021 fire as an example, Figure 3).

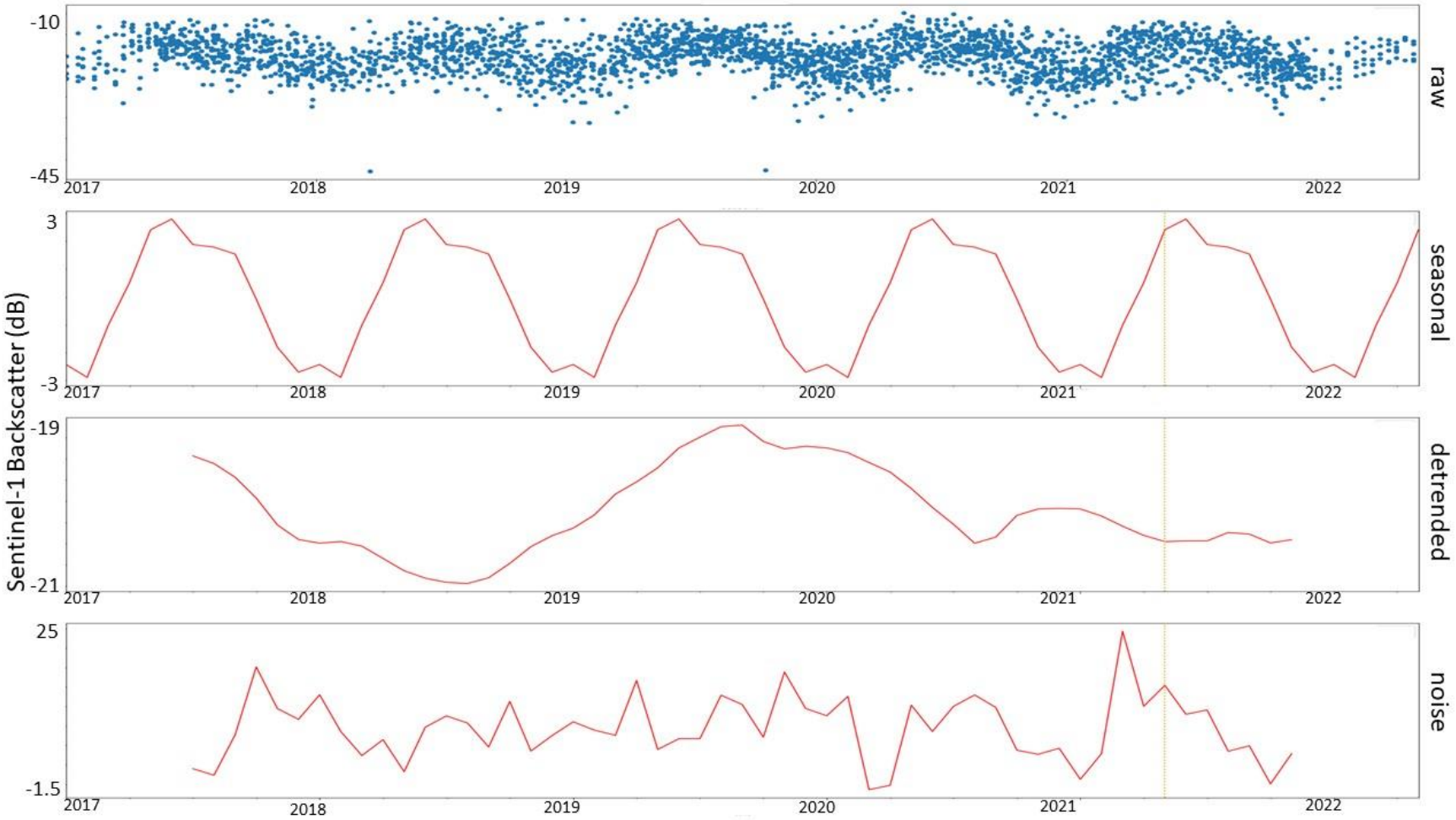

Figure 1: Example of seasonal decomposition of Sentinel-1 VH backscatter at Tomahawk, Alberta fire, which occurred on May 7, 2021. Top panel represents the raw data (SAR VH backscatter); 2nd panel represents seasonal component; 3rd panel represents decomposed trend; Bottom panel represents noise. Orange vertical line represents the date of the fire.

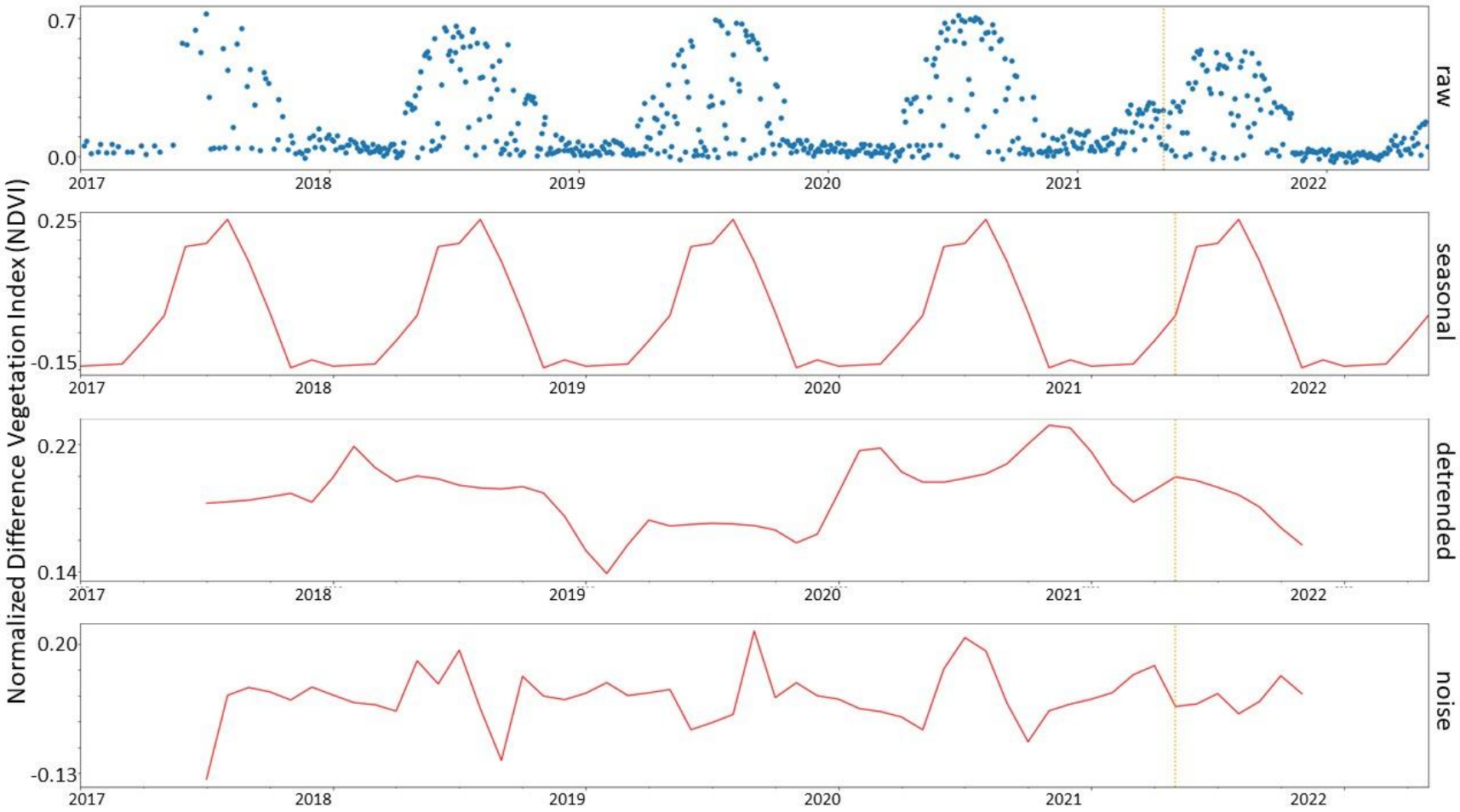

Figure 2: Example of seasonal decomposition of Sentinel-2 NDVI backscatter at Tomahawk, Alberta fire, which occurred on May 7, 2021. Top panel represents the raw data (NDVI); 2nd panel represents seasonal component; 3rd panel represents decomposed trend; Bottom panel represents noise. Orange vertical line represents the date of the fire.

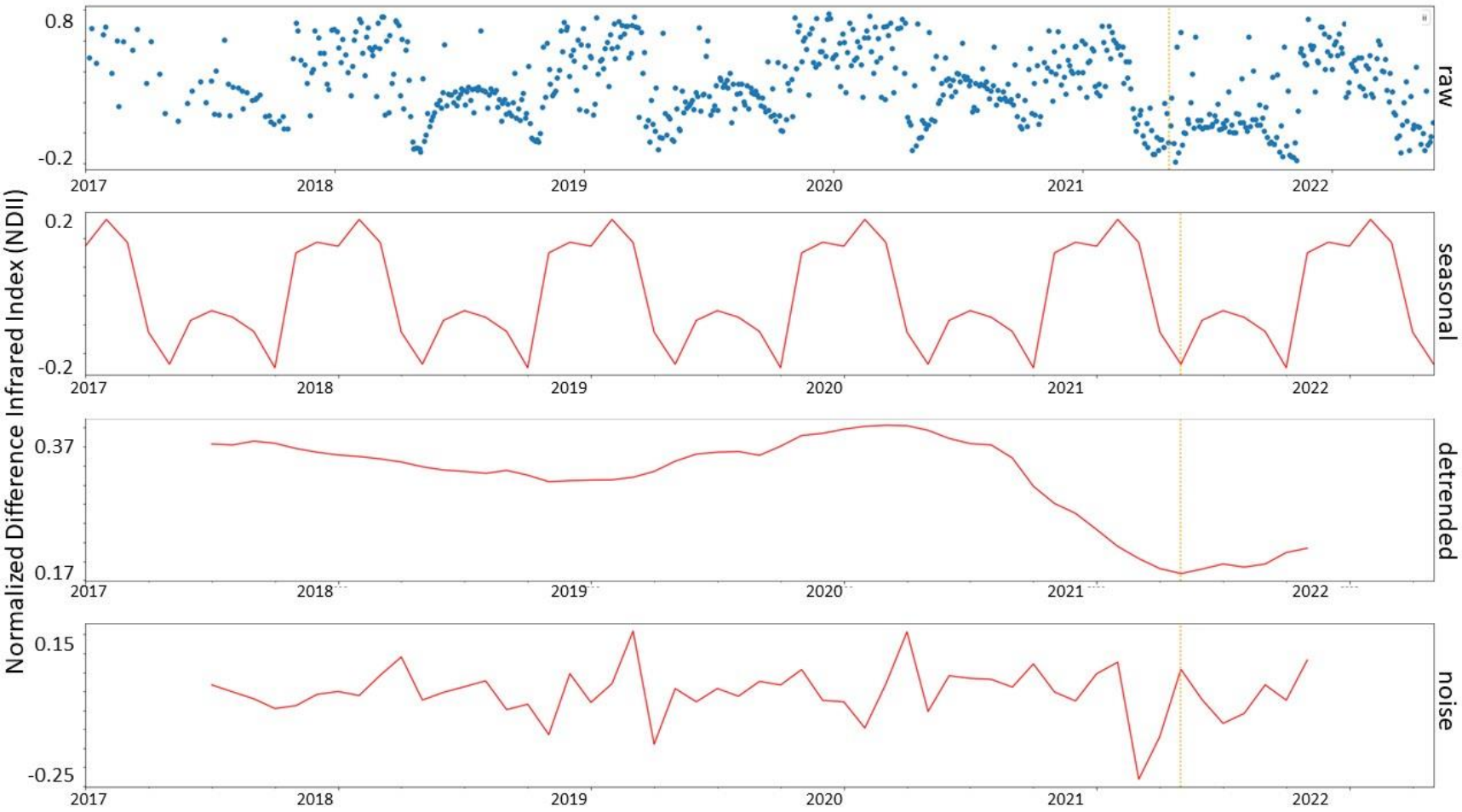

Figure 3: Example of seasonal decomposition of Sentinel-2 NDII backscatter at Tomahawk, Alberta fire, which occurred on May 7, 2021. Top panel represents the raw data (NDII); 2nd panel represents seasonal component; 3rd panel represents decomposed trend; Bottom panel represents noise. Orange vertical line represents the date of the fire.

We hypothesized that surface moisture conditions are reduced prior to a peatland burning (*i.e.*, indicating drought conditions), and this phenomenon will appear as a detectable reduction in SAR backscatter in a seasonally decomposed time series of Sentinel-1. To explore the utility of using Sentinel-1 C-Band SAR backscatter (VV and VH polarizations) as a tool for monitoring wildfire vulnerability in peatlands, we tested several time intervals prior to wildfire to determine if reductions in backscatter could be detected. Ultimately, demonstrating the utility of time-series of Sentinel-1 backscatter in identifying the likelihood of a peatland burning would contribute to the development of an "early warning system" for peatland vulnerability to drought and wildfire. However, a peatland can enter into drought conditions and not burn simply because there is no point of ignition (*e.g.*, no lightning strikes or transfer from upland wildfires). For comparison we also tested the utility of Sentinel-2 indices in detecting trends in time series prior to wildfires. Based on these premises and using both Sentinel-1 and Sentinel-2, the objectives of this research were to:

1) Determine at which specific time periods prior to a fire statistically significant trend slopes exist in seasonally decomposed time series data.
2) Determine if there is a difference between the *direction* and *magnitude* of slopes of decomposed time series in burned and unburned peatlands at specific time periods prior to a fire.

2. Methods

Peatlands throughout Canada's Boreal Forest (Figure 4) were sampled using the peatland extent dataset from Thompson *et al.*,(2016). From this dataset, we randomly selected 10000 random locations that were estimated with greater than 80% probability to be representative of peatlands.

We also sampled an additional 1600 points from a dataset comprised of validated peatland sites from various sources (Bona *et al.,* 2018; Bourgeau-Chavez *et al.,* 2019; Dieleman *et al.,* 2020; Errington *et al.,* 2020; Gibson *et al.,* 2021; Mansuy *et al.,* 2014; "Passive Control Networks," 2022; Thompson *et al.,* 2017) including unpublished data from field campaigns at the DeBeers' Victor Mine in Northern Ontario in 2011-2013 and interpretation of aerial photographs from Wood Buffalo National Park in Northern Alberta and southern Northwest Territories (2015). This resulted in a total sample size of 11600 "probable peatland" sample locations. As the sample is mainly based on the Thompson *et al's (2016)* peatland probability grid. The samples are spaced a minimum of 250 m apart (Figure 4).

Sentinel-1 Interferometric Wide Mode (Sentinel-1) and Sentinel-2 Top of Atmosphere Level 1 (Sentinel-2) data were accessed using Google Earth Engine (Gorelick *et al.,* 2017). Sentinel-1 data were masked to exclude data that coincided with large water bodies and data below the noise floor (-22 dB), then a Lee filter was applied to reduce speckle noise (Lee *et al.,* 1994). Sentinel-2 data were cloud masked and two indices found useful for peatland vegetation and wetness assessments were calculated: Normalized Difference Vegetation Index (NDVI) (Arroyo-Mora *et al.,* 2018; Artz *et al.,* 2019) and Normalized Difference Infrared Index (NDII) (Neta *et al.,* 2010). The median Sentinel-1 VV and VH backscatter, as well as the median Sentinel-2 NDVI and NDII indices, were calculated for a 50 m area around each sample site at each available date between January 1, 2017, and January 1, 2022.

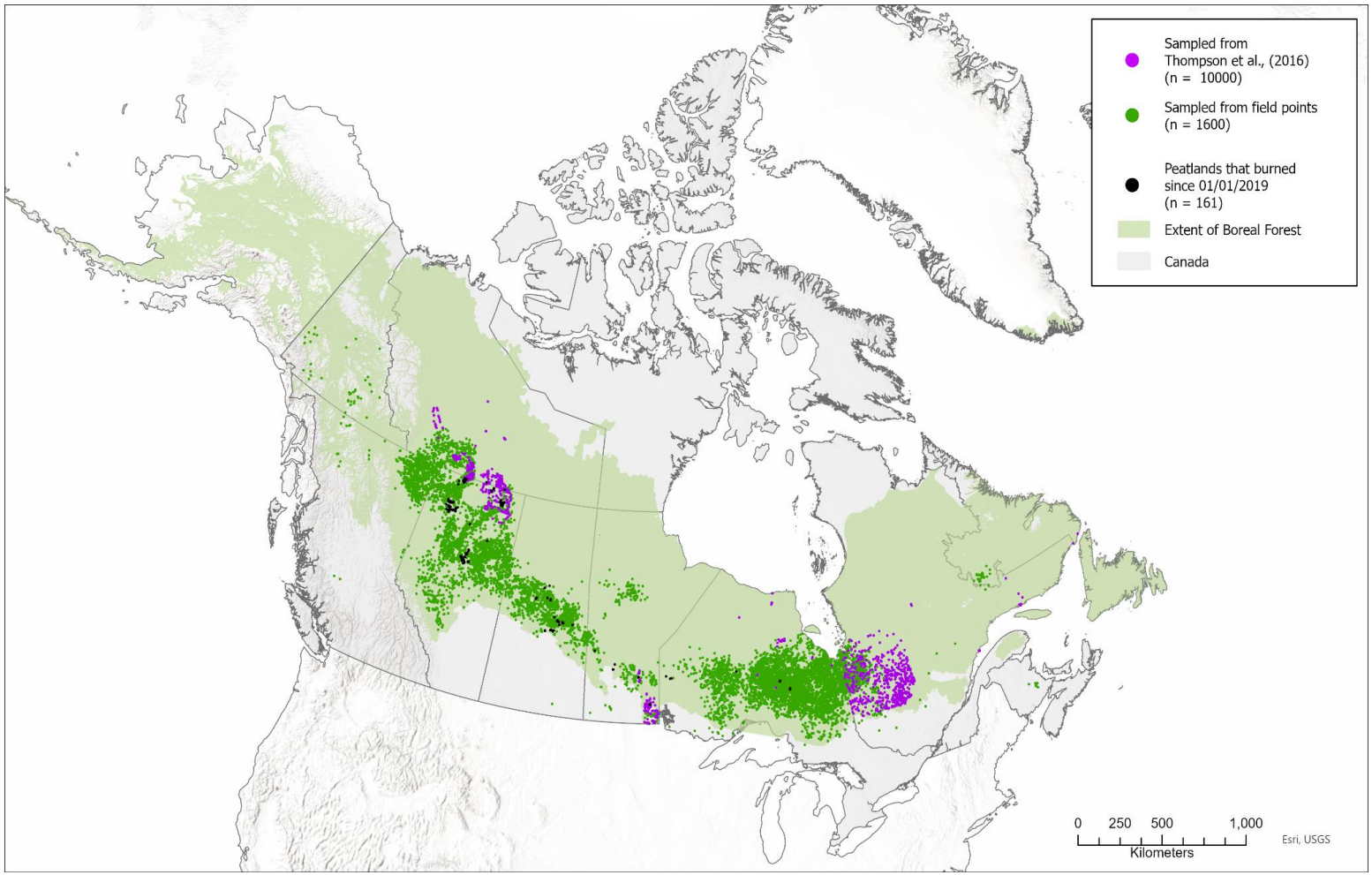

Figure 4: map of Canada indicating where samples are located and extent of boreal forest (light green). Purple samples are validated peatland sites derived from the following sources: (Bona *et al.*, 2018; Bourgeau-Chavez *et al.*, 2019; Dieleman *et al.*, 2020; Errington *et al.*, 2020; Gibson *et al.*, 2021; Mansuy *et al.*, 2014; "Passive Control Networks," 2022; Thompson *et al.*, 2017). Green samples are from (Thompson *et al.*, 2016). Black samples are those that burned between Jan 1, 2019 and December 31, 2021.

The peatland sample location data were spatially intersected with the National Burned Area Composite Dataset (NBAC) (Hall *et al.,* 2020) to identify sites that had experienced fire between 2019 and the end of 2020 (the last available date of the NBAC). Sites that burned between 2017 and 2019 were excluded as the length of the time series produced using Sentinel-1 and Sentinel-2 data is too short to obtain high quality estimates of seasonally decomposed time series. For the 2021 fire season, "fire progression" polygons derived from the Canadian Wildland Fire Information Fire M3 hotspots dataset (Canada, 2022; Fraser *et al.,* 2000) were used to estimate fire extents. Any site that fell within a fire extent polygon was considered a "burned" site and the date of the fire was recorded. Any site that had burned prior to 2017 was excluded from further analysis, and any site that did not experience fire was considered "unburned".

As several Sentinel-1 orbits (*i.e.,* track and pass) cover each sample either fully or partially throughout the year, the most frequent pass/track combination was selected for each site for further analysis. As some sites were imaged every 6 days and some every 12 days, the data were interpolated to a regularly spaced time series at a weekly temporal resolution using Kalman Smoothing interpolation (Harvey, 1990), an interpolation technique specifically designed for interpolating gaps in time series data. The *Classical Seasonal Decomposition by Moving Averages* technique (R: Classical Seasonal Decomposition by Moving Averages, 2022), using additive decomposition, was applied to separate the seasonal component of the data from the noise and trend. For burned sites, the trend was extracted for specific time periods (6 weeks, 3 months, 6 months, 12 months, 18 months) before the fire and the Theil-Sen slope (Mariano *et al.,* 2018; Sen, 1968) of the trend was calculated for each time period. Theil-Sen is a non-parametric technique for computing the slope of a Mann-Kendall trend in time series data (Mann, 1945). For

the unburned sites, as no “burned date” exists, the same procedure was followed, but using a random date between May 15 and Aug 15 of the years 2019 - 2021.

As there were many more unburned sites (n = 11447) than burned sites (n = 161), unburned sites were split randomly into equally sized groups (n = 161 each, 71 groups). A Kruskall-Wallis (Kruskal and Wallis, 1952) test was run in a bootstrapped manner (71 unique bootstrap samples) to identify significant differences in Theil-Sen slope between the set of burned sites with each group of unburned sites. Additionally, to determine if there was a significant difference in the number of positive or negative Theil-Sen slopes between the groups, the number of significant positive and significant negative slopes was counted at burned sites and each set of unburned sites. These counts were compared using bootstrapped Chi-Squared (Pearson, 1900) tests, with Bonferroni correction (Armstrong, 2014) applied based on the number of bootstrapped tests.

Preliminary tests of the methodology across a large, continuous area (for spatial mapping purposes), including seasonal decomposition and Theil-Sen slope calculations, were performed on a known peatland fire in Tomahawk, Alberta, that occurred in early May, 2021. The fire extent was approximately 21 square km, covering a mix of upland forest, peatland and mined peatlands. The peatland portions of the fire were primarily smoldering, with significant effects on regional air quality.

3. Results

From a few example peatland fires (*e.g.,* Tomahawk, AB), preliminary testing indicated a clear seasonal trend in both Sentinel-1 backscatter and Sentinel-2 indices (NDVI and NDII). Using the Classical Seasonal Decomposition by Moving Averages technique, both Sentinel-1

backscatter and Sentinel-2 NDII showed a decrease in magnitude (negative slope) of the trend component immediately prior to a fire, however NDVI's trend component did not exhibit a clear decrease or increase (Figures 1, 2 and 3).

3.1 Comparison of Sentinel-1 trend Theil-Sen slopes between burned and unburned peatlands

The calculated Theil-Sen slope is indicative of the trend in S1 backscatter over the time period. A negative Theil-Sen slope represents a decrease in S1 backscatter over time. As we expect decreasing soil moisture with decreasing backscatter, a negative Theil-Sen slope may indicate a site that is experiencing drying conditions.

There was a significant difference in both VV and VH trend slopes between all groups of burned and unburned peatlands at the 6 month time interval (Kruskal-Wallace test $p < 0.05$) for all bootstrapped groups, and at the 3 month time interval for most groups (66 and 67 out of 71 for groups for VV and VH, respectively; Table 1). At both the 12 and 18 month time periods, VH showed no statistically significant differences ($p > 0.05$). Similarly, the majority of groups were not significantly different in VV at these time periods. Time periods shorter than 3 months (*e.g.,* 6 weeks) resulted in no significant Theil-Sen slopes. Visual interpretation of boxplots and probability distributions of these groups indicated that at 3 and 6 months prior to a fire, burned sites had lower and more negative slopes than unburned sites, although there is overlap in the distributions (Figures 5 and 6). This means that between 3 and 6 months prior to a wildfire, the slope of decomposed S1 data could be useful in detecting the vulnerability of a peatland to ignition. The VV polarization resulted in a stronger distinction, visually, between burned and unburned sites, though both polarizations (VV and VH) appear similar through Kruskal-Wallace tests. We can see that at all time periods there is significant overlap in the data distribution

between burned and unburned sites (Figures 5 and 6). However, the magnitude of the VV Theil-Sen slope continually reduces (*i.e.,* becomes more negative) leading up to the fire (Figure 6).

Table 1: Difference of Theil-Sen slopes values in burned and unburned sites for seasonally-decomposed VV and VH polarizations over specific time periods. P-values represent significance of Kruskal-Wallace test: where result is significant ($p < 0.05$), burned and unburned sites had different Theil-Sen slopes on decomposed data (*e.g.,* burned sites were more negatively-trending slopes than unburned sites). Significant differences highlighted with an Asterix (*) .

VV	**VH**	**Time Period**
68 of 71 $p > 0.05$	All $p > 0.05$	18 months
41 of 71 $p > 0.05$	All $p > 0.05$	12 months
0 $p > 0.05$*	0 $p > 0.05$*	6 months*
5 of 71 $p > 0.05$*	4 of 71 $p > 0.05$*	3 months*
No significant Theil-Sen slopes (*i.e.,* $p > 0.05$)	No Significant Theil-Sen slopes (*i.e.,* $p > 0.05$)	6 weeks

Table 2: Results of chi-squared test, comparing the counts of positive and negative Theil-Sen slopes in burned and unburned peatlands. Where the result is significant ($p < 0.05$), burned and unburned sites had different counts.

VH positive	**VH negative**	**VV positive**	**VV negative**	**Trend Period**
All $p > 0.05$	All $p > 0.05$	All $p > 0.05$	All $p > 0.05$	18 months
All $p > 0.05$	All $p > 0.05$	All $p > 0.05$	All $p > 0.05$	12 months
0 $p > 0.05$*	All $p > 0.05$	0 $p > 0.05$*	All $p > 0.05$	6 months*
6 of 71 $p > 0.05$*	All $p > 0.05$	10 of 71 $p > 0.05$*	All $p > 0.05$	3 months*

To visually assess the consistency of Theil-Sen slopes between burned and unburned sites, the trends of all burned sites (n = 161) and the VV polarization trends of a sample (n = 161) of unburned sites were plotted against the number of days prior to ignition (Figure 7). In the case of unburned sites, the random date assigned to each site was used to simulate the “time since fire”.

Using a relative time scale based on “time since fire” (*i.e.* number of days prior to a fire) allows us to visualize the Theil-Sen slopes of burned sites for direct comparison. Burned sites tend to show negative slopes at 3 and 6 months before a fire, while overall trends vary at 12 and 18 months pre-fire (Figure 7). Quantitatively comparing the counts of positive and negative slopes (Chi-square test), there were significant differences in the number of positive trends in burned and unburned sites for both VV and VH, with burned sites resulting in far fewer positive slopes (Table 2). At 3 months prior to a fire, most burned and unburned sites were significantly different (6 of 71 for VV and 10 of 71 for VH were not significant), and for 6 months, all were significantly different. At both 3 and 6 months, burned sites had primarily negative slopes, whereas unburned sites had both negative and positive slopes. Unburned sites experience both positive and negative trends, indicating that some unburned sites may also be experiencing drying or drought but did not burn.

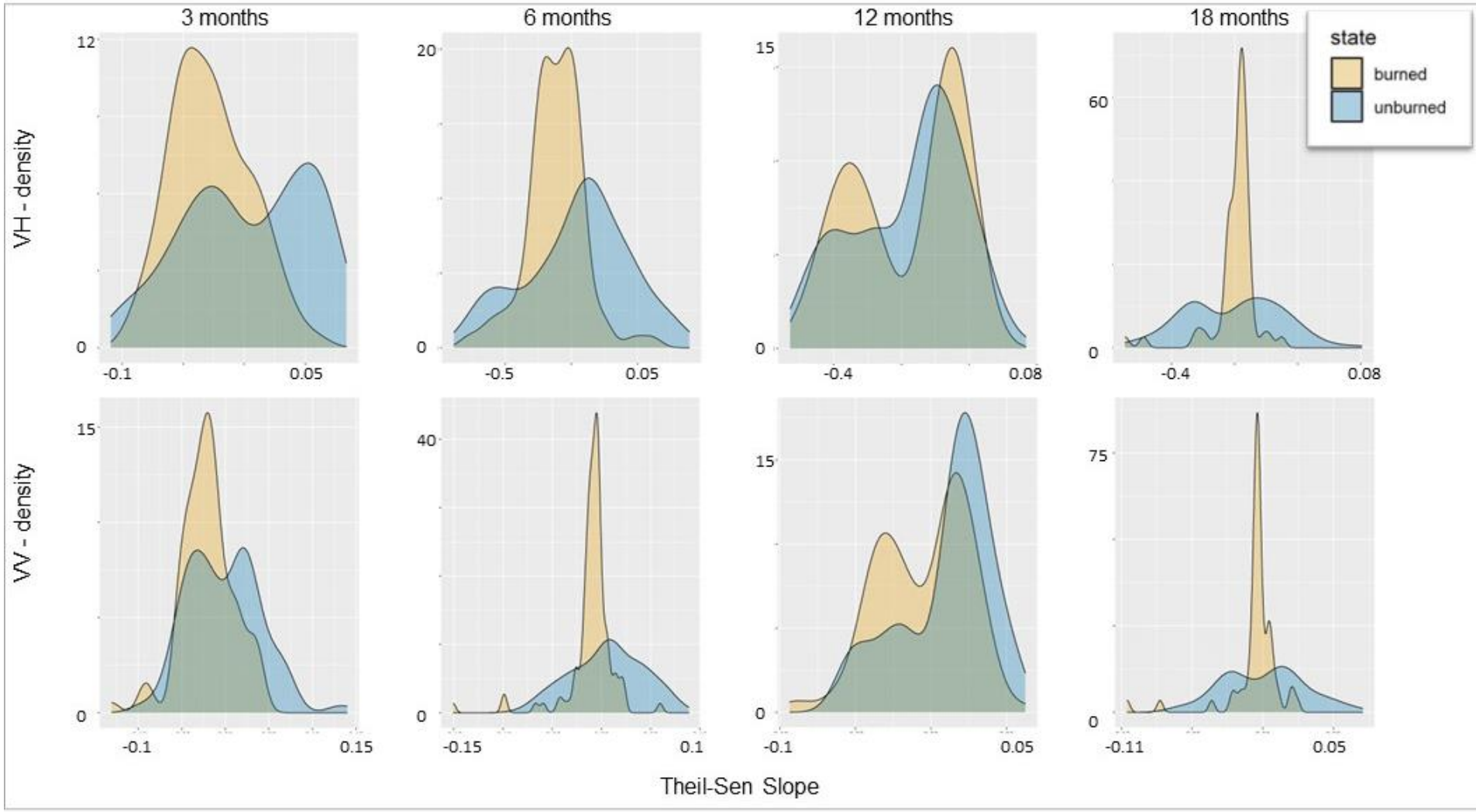

Figure 5: shows the probability density distributions for Theil-Sen slopes of decomposed data (VV and VH) trends in burned and unburned sites. Note that VV shows a clearer distinction between burned and unburned sites at both 6 months and 18 months prior to a fire.

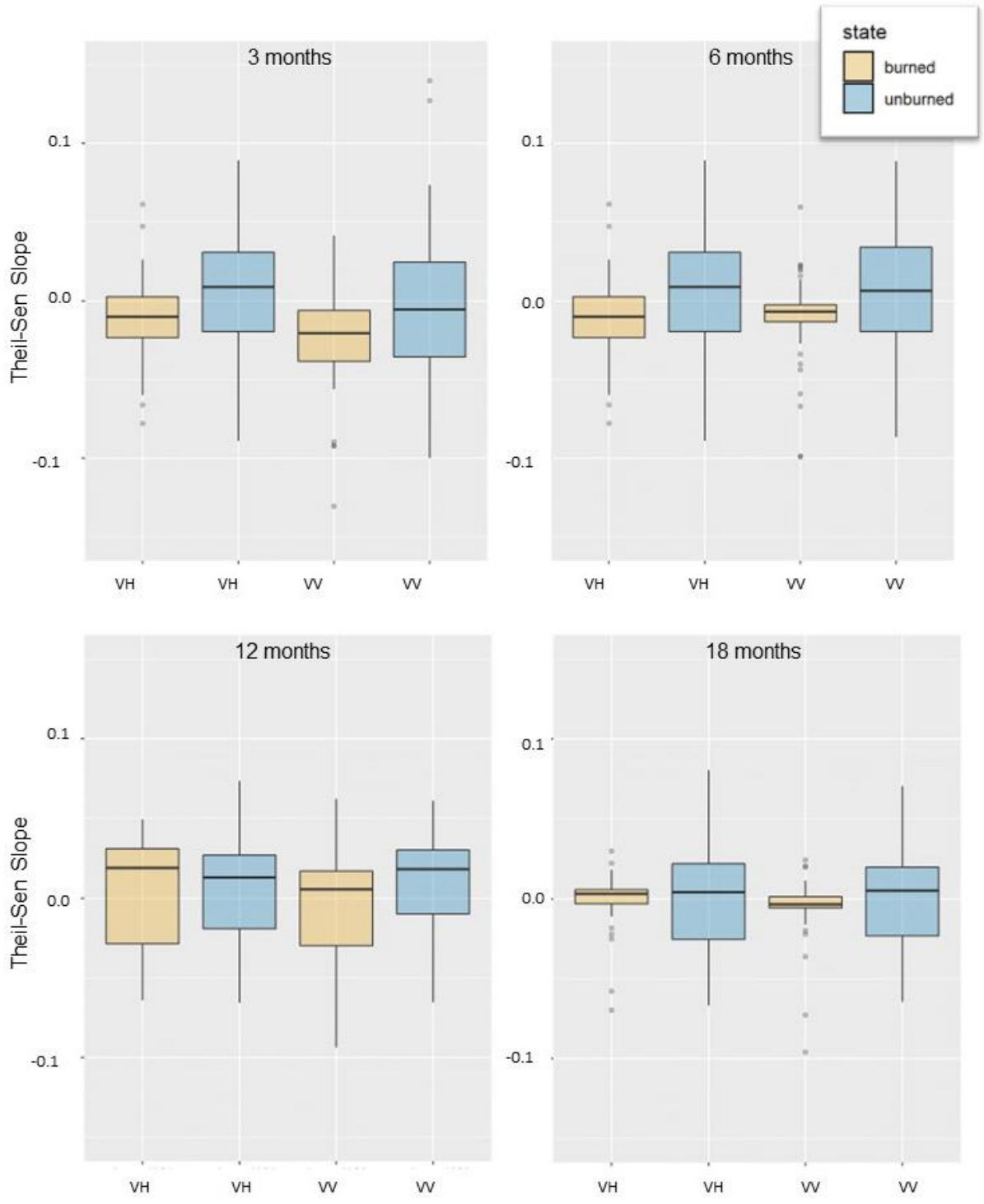

Figure 6: shows boxplots for VV Theil-Sen slopes of decomposed data in burned and unburned sites. Note that at 6 and 3 months prior to fire, the burned sites exhibit primarily negative slopes (interquartile range is fully negative), but at all time intervals there are some positive slopes present.

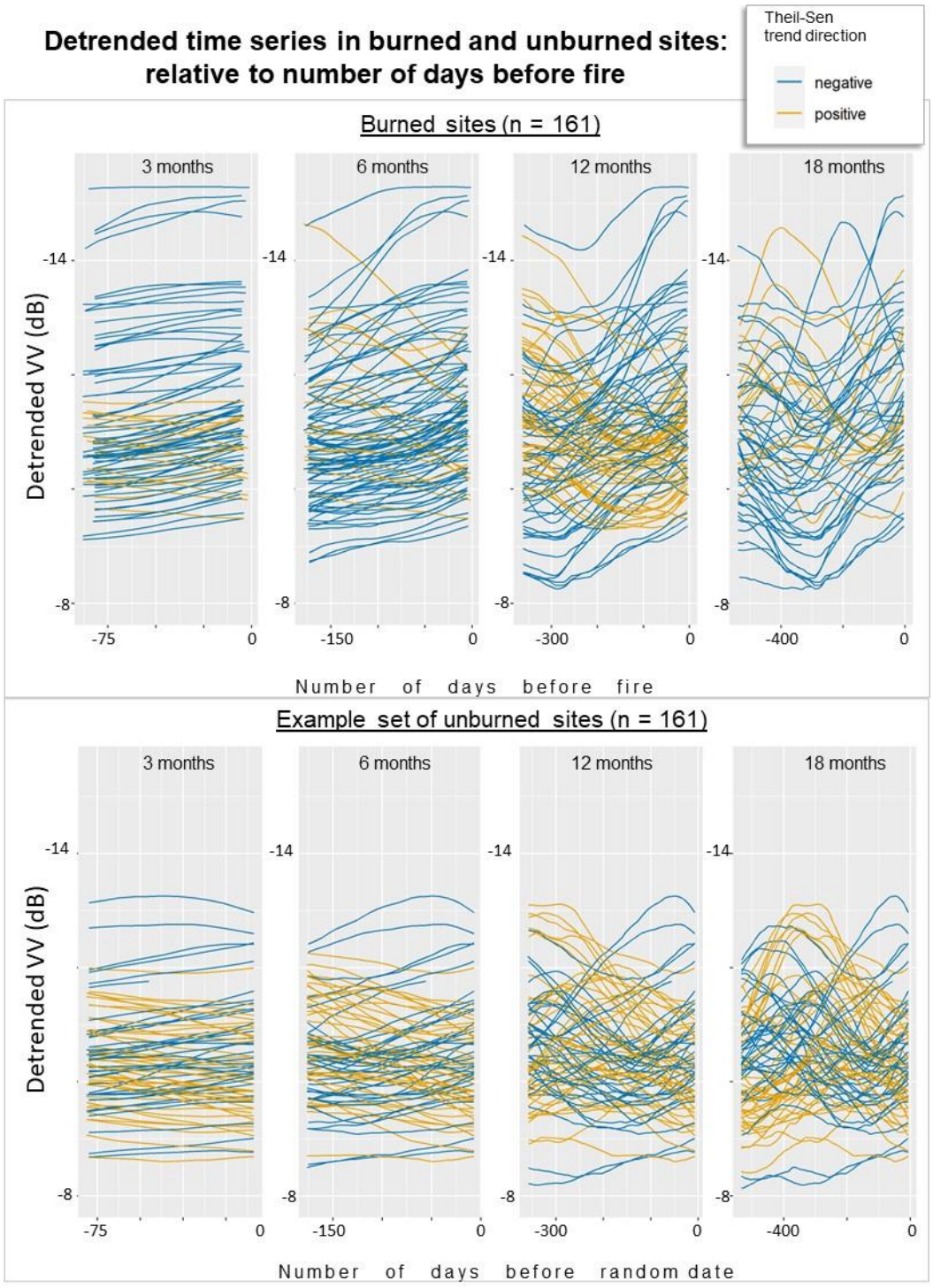

Figure 7: shows decomposed time series in burned peatlands (top) and an example of unburned peatlands (bottom), coloured by trend direction at various time periods. At times closer to the fire (e.g. 3 and 6 months before), we see mostly negative trends in burned sites and a mixture of decreasing and increasing in unburned sites. At 12 and 18 months prior to a fire, trends often are highly variable in both burned and unburned sites indicating that some of the unburned sites might not be experiencing detectable drought this far in advance of a fire.

3.2 Comparison of Sentinel-2 trend slopes in burned and unburned peatlands

Surprisingly, none of the slopes were significantly different (Kruskal-Wallace $p < 0.05$) between burned and unburned sites using either Sentinel-2 NDVI or NDII decomposed time series (Table 3). Additionally, in chi-squared tests, there were no significant differences between the burned sites and any of the groups of unburned sites in the count of positive or negative slopes (Table 4). Although our preliminary tests at a few known peatland sites showed that NDII decreased immediately before a fire, using all 11600 samples, results were not statistically significant, indicating that the Theil-Sen slopes of decomposed Sentinel-2 NDVI and NDII may not be suitable for assessing vulnerability to wildfire within peatlands, when all types of peatlands are considered.

Table 3: shows the number of Kruskall-Wallace comparisons where NDVI and NDII Theil-Sen Slopes were significant for each time periods.

NDVI	**NDII**	**Time Period**
All $p > 0.05$	All $p > 0.05$	18 months
All $p > 0.05$	All $p > 0.05$	12 months
All $p > 0.05$	All $p > 0.05$	6 months
All $p > 0.05$	All $p > 0.05$	3 months
No significant Theil-Sen slopes (*i.e.,* Theil-Sen $p > 0.05$)	No Significant Theil-Sen slopes (*i.e.,* Theil-Sen $p > 0.05$)	6 weeks

Table 4: shows the number of chi-square test comparisons where positive and negative slope counts were different in NDVI and NDII trends for each time period.

NDVI positive	**NDII negative**	**NDVI positive**	**NDII negative**	**Trend Period**
All $p > 0.05$	All $p > 0.05$	All $p > 0.05$	All $p > 0.05$	18 months
All $p > 0.05$	All $p > 0.05$	All $p > 0.05$	All $p > 0.05$	12 months
All $p > 0.05$	All $p > 0.05$	All $p > 0.05$	All $p > 0.05$	6 months
All $p > 0.05$	All $p > 0.05$	All $p > 0.05$	All $p > 0.05$	3 months

3.3 Assessing the spatial variability of trends

Calculating the decomposed time series for the Tomahawk, Alberta, 2021, fire indicates strong spatial patterns in Theil-Sen slope at the 3, 6 and 12 month time periods before the fire. At 18 months before the fire, there are no strong patterns and many of the slopes are not significant ($p > 0.05$). It is clear from comparison of spatial time intervals that sections of the mined peatlands show earlier and more negative slopes than surrounding treed bog and upland forests. It is also clear that areas outside the fire extent also experienced negative slopes prior to the fire.

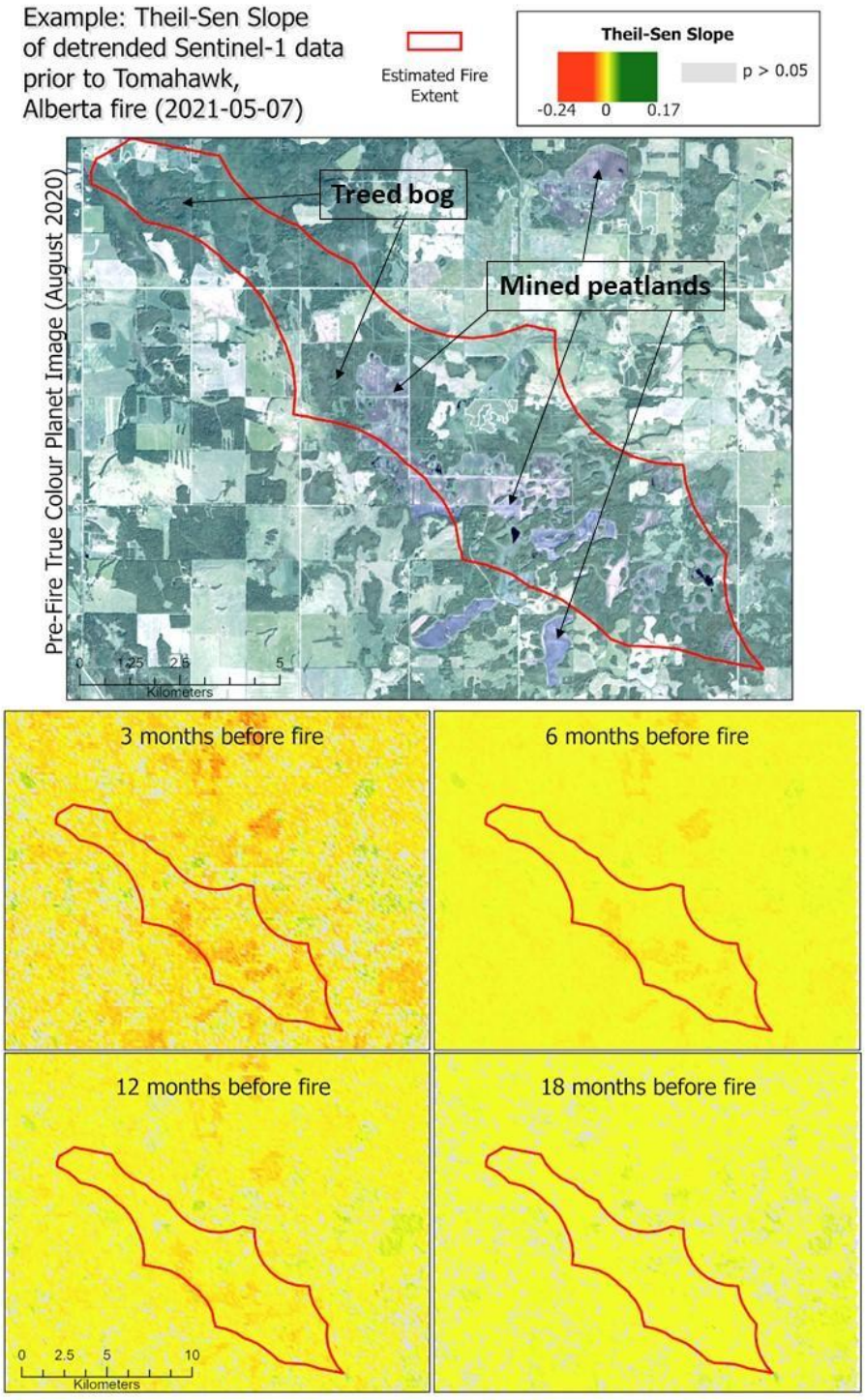

Figure 8: Top panel shows the general study area with fire extent outlined in red, and a pre-fire true colour PlanetScope image is displayed in the background. The bottom four panels show spatial maps of trends at different time periods prior to the Tomahawk, AB fire, which occurred on May 7, 2021. Positive slopes are in red and negative slopes are in green. Yellow represents when no slope is present (slope = 0).

4. Discussion

Fire management agencies currently lack tools to monitor changing surface conditions in boreal peatlands. In other ecosystems (*e.g.*, upland forests), remote sensing has integrated information about vegetation conditions, and has focused on predicting the probability of wildfire occurrence. While vascular vegetation in peatlands does undergo stress due to drought and drying (McPartland *et al.,* 2019), they are often sparsely vegetated with vascular plants, so a better indicator of drought is the surface conditions of mosses. NDII has been shown to be related to peatland surface moisture conditions (Mirmazloumi *et al.,* 2021; Neta *et al.,* 2011, 2010), whereas NDVI has been found to be related to variability in density of vascular vegetation and Leaf Area Index (Harris, 2008; Juutinen *et al.,* 2017; McPartland *et al.,* 2019; Zheng and Moskal, 2009). We did not test the differences in static NDVI or NDII products for differences in burned and unburned areas prior to fires. In our analysis, although the overall Theil-Sen trends in NDVI and NDII were found to be significant, we found no significant differences between the NDVI or NDII trends in burned and unburned sites at any time period prior to a fire.

As C-Band SAR is sensitive to variability in vegetation structure, vegetation water content and soil moisture, a reduction in VV backscatter could be attributed to changes in any of those components. Past studies using SAR primarily examined the relationship between SAR backscatter and either fuel moisture, soil moisture or fire danger ratings (e.g. Bourgeau-Chavez et al., (1999), Leblon et al., (2002), Bourgeau-Chavez et al., (2007), and Abbott et al., (2007)). In this research we focus on interpreting the trends over time in SAR backscatter, and do not aim to predict an specific variable such as soil moisture, fuel moisture or biomass, but assess the general changes over time in the composite backscatter signal (i.e. the backscattered signal

comes from the surface and vegetation). Through seasonal detrending Sentinel-1 time series, we remove both the noise and seasonal components of the signal. The seasonal component of the signal is likely related to changes in vegetation phenology and normal wetting and drying cycles over a growing season. The remaining trend component indicates deviations from the normal phenologic and hydrologic conditions, and can reveal instances of multi-year drought or increases in wetness over time, providing an indicator of sustained changes in hydrologic cycles, including drought. Due to the unpredictable nature of wildfire ignitions, we cannot definitively predict if a peatland will burn based on surface conditions alone (*i.e.*, we will identify false positives). Based on the method developed in this research, we can indicate areas that may be experiencing changes in surface conditions (*e.g.*, drought) and are at risk of ignition, should an ignition source be introduced. Our analysis indicates that the spatial and temporal response (*i.e.*, trend) of Sentinel-1 backscatter to such changes may be sufficient to identify peatland areas that have entered a period of extended drying and therefore wildfire vulnerability. This information may provide fire management agencies a supplemental tool to monitor peatland drought conditions and wildfire vulnerability.

Unlike NDVI and NDII, based on the 11600 peatlands sampled, we did find reduced Sentinel-1 backscatter prior to fires at burned peatland sites. While trends in NDVI and NDII were significant, they may be less precise than the trends derived from SAR due to missing dates due to cloud. In these cases, missing dates were interpolated based on prior values, potentially skewing trend results. SAR is insensitive to clouds and therefore data can be acquired consistently (*e.g.*, every 12 days), reducing the effects of and reliance on a single date in interpolation. As noted above, a reduction in SAR backscatter has been shown to be related to

reduced surface wetness, reduced vegetation water content or change in vegetation composition and structure over time. These findings could indicate either that vegetation has not been significantly affected by changes in surface wetness conditions or that burned and unburned peatlands are experiencing the same changes in vegetation.

We did not remove snow covered images from our analysis because the time series method used here requires continuous data for the entire time series. Whereas we were able to interpolate between cloudy images, snow covered images cover a larger continuous portion of the year at our sites (e.g. November through April in some cases). Leaving snowy images in the time series allows the snow signal to be extracted in the seasonal component of the signal, assuming the snow conditions and timing of snow stayed consistent over the time series. For example, if the snow was becoming continually wetter over time, this portion of the snow signal would be captured in the trend signal. Or, if snow conditions were occurring later in the fall each year, this change would likely be captured as noise in the time series method used here. However, it should be noted that the effect of dry winter conditions and low snow cover alone do not necessarily result in drought conditions and increased wildfire susceptibility in all boreal peatlands (e.g. Elmes et al, 2018). The "synchronization" of low previous fall soil moisture, modest or low snowfall conditions, low spring rainfall amounts, above-average spring air temperatures and high winds result in the years with largest boreal peatland burn area (Elmes et al, 2018). Many boreal peatland fires are able to smolder over winter and reignite as a surface fire immediately after snowmelt. The effect of snow (timing of snow cover, snow water equivalent), and conditions immediately prior to and following snow melt should be further investigated in a wide variety of boreal peatlands.

Spatial estimates of trends at the Tomahawk, Alberta site revealed interesting patterns in the landscape. It is important to note that 6 months prior to the fire, much of the burned area has a Theil-Sen slope near zero (yellow in Figure 8), except for a few areas within the burned area polygon. It was clear that these areas with negative slopes (red areas in Figure 8) are disturbed peatlands, and they exhibited the clearest signal in reduced backscatter over time. This could be because these areas are fully open (*i.e.*, unvegetated) and therefore, noise due to vegetation was eliminated. However, it also could be because these areas are no longer functioning peatlands and are unable to hold surface soil moisture, making them generally more vulnerable to drought and therefore at risk of burning and smoldering if an ignition source is introduced. Generally, we can see that 3 months prior to the fire, most of the landscape surrounding the burned area was exhibiting negative Theil-Sen slopes. The Tomahawk fire was contained by Fire Management Agencies, so the extent of burn could have been much greater. It is also important to note that 6 months prior to the fire, the general area exhibited significant Theil-Sen slopes ($p < 0.05$), whereas at all other time periods assessed, there were many pixels that exhibited non-significant slopes ($p > 0.05$).

While working with single time series for each of the 11600 sampled probable peatland locations was relatively quick to process, producing spatial (*i.e.*, raster) estimates of time series slopes was time consuming on a high end desktop computer (Ryzen 3090ti processor, 128 GB ram). Scripts were developed in R Statistics Software and parallelized across 29 cores, but analysis for an 260 square kilometer area required more than 6 hours of processing (203 x 103 pixels at 100 m pixel spacing; resampled from original 10 m pixel spacing). If this method were to be adopted

operationally for Fire Management Agencies, it would be necessary to further reduce pixel size, sample large areas sparsely, or use a supercomputer for processing.

4.1 Limitations and Future Work

The Classical Seasonal Decomposition by Moving Averages technique has several limitations. First, since the technique relies on the calculation of a moving average, and the estimate of the trend-cycle cannot be computed for the first few and last few observations. For example, if m = 12 (monthly data), there is no trend-cycle estimated for the first six or the last six observations (*i.e.*, months). Second, this detrending technique is not sensitive to abrupt changes ("spikes" or "dips") in the time series so very rapid changes are not captured in the decomposed time series. This could mean that when a peatland experiences rapid environmental change (*e.g.*, drainage), the resulting reduction in S1 backscatter will not be detected. Third, this method assumes that the seasonal signal is consistent year to year. This may not be true, especially due to climate change where snow melt is occurring earlier, greening is peaking at different times, and freeze up occurs later (Hyndman and Athanasopoulos, 2018).

The Theil-Sen calculation of slope also has limitations. Although it is non-parametric (*i.e.*, doesn't assume data are independent, and is therefore valid for time series analysis), this technique tests for *linear* trends. In some cases, the trend may not be linear. For example, Theil-Sen assumes that the "overall" trend is monotonic (consistently decreasing or increasing, either negative or positive), but at longer time periods, trends are not necessarily monotonic (they may increase then decrease). In these cases, Theil-Sen slope will estimate the trend as being either positive or negative. Trends that are not found to be monotonic will be non-significant ($p>0.05$). In the case of longer time periods, a sensitivity analysis should be completed based on a moving-

window of time, rather than wide, discrete intervals tested here (*e.g.*, test trends at intervals of 1 month rather than at 6, 12 and 18 months only).

While time series of C-Band SAR have been shown to be a useful tool for monitoring peatland surface conditions, the continuity of the SAR time series datasets is important to consider. In December 2021, the Sentinel-1B satellite of the Sentinel-1 constellation failed and has not successfully collected data since (European Space Agency, 2022). This will certainly have an effect on time series analysis by introducing a large gap in data in many regions. For example, most of central and eastern Canada was previously only covered by Sentinel-1B and therefore any droughts that occur in the 2022 fire season will not be able to be detected using the method presented here. However, most of western Canada (and many other places globally) is imaged regularly with Sentinel-1A and, while the frequency of available imagery will be reduced, time series will still be a viable option for analysis.

While previous research has demonstrated machine learning methods to predict wildfire probability using a variety of GIS and spatial data, the method developed through this work presents the first analysis of differences between Sentinel-1 time series trends in burned and unburned peatlands. Based on the differences evident in this analysis, future work should assess multivariate machine learning approaches to predict the probability of wildfire that include Sentinel-1 backscatter trends as a variable alongside information about vegetation variability, proximity to infrastructure and disturbances, and peatland class.

5. Conclusion

Fire management agencies require information about near-real time wildfire vulnerability in boreal peatlands. Currently, remote sensing tools to monitor changing wildfire vulnerability mainly focus on monitoring changes in vascular vegetation and are not necessarily applicable to moss-dominated peatlands. We use time series analysis of Sentinel-1 SAR data to compare the trends in peatlands that have burned to unburned peatlands, and show that the Theil-Sen slopes of seasonally decomposed SAR backscatter reflects prolonged drought conditions that can lead to wildfire. Overall, we found that 6 months prior to a wildfire the slope of decomposed Sentinel-1 VV SAR was significantly different in burned and unburned peatlands, and can be used to spatially identify fire vulnerability and identify fire-prone areas. This information could be used alongside fire weather data currently used by fire management agencies to delimit fire-ban areas and orient fire suppression efforts. To obtain estimates of fire probabilities in peatlands, future modelling approaches should consider fire vulnerability information obtained from Theil-Sen slopes of decomposed SAR data in addition to information about ignition sources, disturbances, vegetation types and vegetation change. While the method developed here is reliant on continuously-acquired C-Band SAR data, which can be vulnerability to interruptions leading to the acquisition of incomplete time series, and requires heavy computing capabilities for spatial estimates, it offers a near-real time solution for predicting fire vulnerability over large spatial scales.

6. Acknowledgements: We would like to thank Drs. Thompson and Parisien of the Canadian Forest Service for their invaluable ideas and conversations throughout the process of this research. Dr. Thompson is thanked for compiling the field-validated peatland sample. Adam

Mohuiddin is thanked for helping to develop scripts. Natural Resources Canada (Canadian Forest Service) is acknowledged for their generous funding contributions to this research.

7. Description of author's responsibilities: KM conceived the original idea for the analysis, performed literature review, wrote scripts and performed Sentinel-1 data and spatial mapping analysis; SD performed literature review related to Sentinel-2, wrote scripts and performed analysis for Sentinel-2. SS aided in the initial assessment of time series analysis techniques, performed literature review on time series analysis techniques, and interpreted results; NP aided statistical and time series analysis and interpretation of results. All authors contributed to writing and editing the paper.

8. Funding: This work was supported by Natural Resources Canada's (Canadian Forest Service) Emergency Management Strategy Wildfire Component R&D grants [grant numbers FIRENFC-24 and FIRENFC-18] and Carleton University [grant number 186207].

References

Abbott, K.N., Leblon, B., Staples, G.C., Maclean, D.A., Alexander, M.E., 2007. Fire danger monitoring using RADARSAT-1 over northern boreal forests. Int. J. Remote Sens. 28, 1317–1338. https://doi.org/10.1080/01431160600904956

Akther, M.S., Hassan, Q.K., 2011. Remote Sensing-Based Assessment of Fire Danger Conditions Over Boreal Forest. IEEE J. Sel. Top. Appl. Earth Obs. Remote Sens. 4, 992–999. https://doi.org/10.1109/JSTARS.2011.2165940

Armstrong, R.A., 2014. When to use the Bonferroni correction. Ophthalmic Physiol. Opt. 34, 502–508. https://doi.org/10.1111/opo.12131

Arroyo-Mora, J.P., Kalacska, M., Soffer, R., Ifimov, G., Leblanc, G., Schaaf, E.S., Lucanus, O., 2018. Evaluation of phenospectral dynamics with Sentinel-2A using a bottom-up approach in a northern ombrotrophic peatland. Remote Sens. Environ. 216, 544–560. https://doi.org/10.1016/j.rse.2018.07.021

Artz, R.R.E., Johnson, S., Bruneau, P., Britton, A.J., Mitchell, R.J., Ross, L., Donaldson-Selby, G., Donnelly, D., Aitkenhead, M.J., Gimona, A., Poggio, L., 2019. The potential for modelling peatland habitat condition in Scotland using long-term MODIS data. Sci. Total Environ. 660, 429–442. https://doi.org/10.1016/j.scitotenv.2018.12.327

Attema, E.P.W., Ulaby, F.T., 1978. Vegetation modeled as a water cloud. Radio Sci. 13, 357–364. https://doi.org/10.1029/RS013i002p00357

Bajocco, S., Dragoz, E., Gitas, I., Smiraglia, D., Salvati, L., Ricotta, C., 2015. Mapping Forest Fuels through Vegetation Phenology: The Role of Coarse-Resolution Satellite Time-Series. PLOS ONE 10, e0119811. https://doi.org/10.1371/journal.pone.0119811

Benscoter, B., Thompson, D., Waddington, J., Flannigan, M., Wotton, M., Groot, W., Turetsky, M., 2011. Interactive effects of vegetation, soil moisture and bulk density on depth of burning of thick organic soils. Int. J. Wildland Fire 20. https://doi.org/10.1071/WF08183

Bisquert, M., Sánchez, J., Caselles, V., 2014. Modeling Fire Danger in Galicia and Asturias (Spain) from MODIS Images. Remote Sens. 6, 540–554. https://doi.org/10.3390/rs6010540

Bona, K.A., Hilger, A., Burgess, M., Wozney, N., Shaw, C., 2018. A peatland productivity and decomposition parameter database. Ecology 99, 2406–2406. https://doi.org/10.1002/ecy.2462

Bourgeau-Chavez, L.L., Garwood, G., Riordan, K., Cella, B., Alden, S., Kwart, M., Murphy, K., 2007. Improving the prediction of wildfire potential in boreal Alaska with satellite imaging radar. Polar Rec. 43, 321–330. https://doi.org/10.1017/S0032247407006535

Bourgeau-Chavez, L.L., Kasischke, E.S., Rutherford, M.D., 1999. Evaluation of ERS SAR data for prediction of fire danger in a Boreal region. Int. J. Wildland Fire 9, 183–194. https://doi.org/10.1071/wf00009

Bourgeau-Chavez, L.L., Battaglia, M.J., Kane, E.S., Cohen, L.M., Tanzer, D., 2019. ABoVE: Post-Fire and Unburned Vegetation Community and Field Data, NWT, Canada, 2018. ORNL DAAC. https://doi.org/10.3334/ORNLDAAC/1703

Canada, N.R., 2022. Canadian Wildland Fire Information System | Data Sources and Methods for Daily Maps [WWW Document]. URL https://cwfis.cfs.nrcan.gc.ca/background/dsm/fm3 (accessed 5.24.22).

Chéret, V., Denux, J.-P., 2011. Analysis of MODIS NDVI Time Series to Calculate Indicators of Mediterranean Forest Fire Susceptibility. GIScience Remote Sens. 48, 171–194. https://doi.org/10.2747/1548-1603.48.2.171

Coogan, S.C.P., Robinne, F.-N., Jain, P., Flannigan, M.D., 2019. Scientists' warning on wildfire — a Canadian perspective. Can. J. For. Res. 49, 1015–1023. https://doi.org/10.1139/cjfr-2019-0094

Damrongkulkamjorn, P., Churueang, P., 2005. Monthly energy forecasting using decomposition method with application of seasonal ARIMA, in: 2005 International Power Engineering Conference. Presented at the 2005 International Power Engineering Conference, pp. 1–229. https://doi.org/10.1109/IPEC.2005.206911

Dieleman, C., Rogers, B.M., Veraverbeke, S., Johnstone, J.F., Laflamme, J., Gelhorn, L., Solvik, K.K., Walker, X.J., Mack, M.C., Turetsky, M.R., 2020. ABoVE: Characterization of Burned and Unburned Boreal Forest Stands, SK, Canada, 2016. ORNL DAAC. https://doi.org/10.3334/ORNLDAAC/1740

Elmes, M., Thompson, D., Sherwood, J., Price, J., 2018. Hydrometeorological conditions preceding wildfire, and the subsequent burning of a fen watershed in Fort McMurray, Alberta, Canada. Natural Hazards and Earth Science Systems. Nat. Hazards Earth Syst. Sci., 18, 157–170

Errington, R.C., Bhatti, J.S., Li, E.H.Y., 2020. Mackenzie Valley Permanent Monitoring Plot Network: a Database of Stand Characteristics. .Information Report NOR-X-428 Canadian Forest Service Northern Forestry Centre.

European Space Agency, 2022. Copernicus Sentinel-1B anomaly (5th update) - Copernicus Sentinel-1B anomaly (5th update) - Sentinel Online [WWW Document]. URL https://sentinels.copernicus.eu/web/sentinel/-/copernicus-sentinel-1b-anomaly-5th-update/1.2 (accessed 6.23.22).

Fraser, R.H., Li, Z., Cihlar, J., 2000. Hotspot and NDVI Differencing Synergy (HANDS): A New Technique for Burned Area Mapping over Boreal Forest. Remote Sens. Environ. 74, 362–376. https://doi.org/10.1016/S0034-4257(00)00078-X

Geudtner, D., Torres, R., Snoeij, P., Davidson, M., Rommen, B., 2014. Sentinel-1 System capabilities and applications, in: 2014 IEEE Geoscience and Remote Sensing Symposium. Presented at the 2014 IEEE Geoscience and Remote Sensing Symposium, pp. 1457–1460. https://doi.org/10.1109/IGARSS.2014.6946711

Ghorbanzadeh, O., Valizadeh Kamran, K., Blaschke, T., Aryal, J., Naboureh, A., Einali, J., Bian, J., 2019. Spatial Prediction of Wildfire Susceptibility Using Field Survey GPS Data and Machine Learning Approaches. Fire 2, 43. https://doi.org/10.3390/fire2030043

Gibson, C., Cottenie, K., Gingras-Hill, T., Kokelj, S.V., Baltzer, J.L., Chasmer, L., Turetsky, M.R., 2021. Mapping and understanding the vulnerability of northern peatlands to permafrost thaw at scales relevant to community adaptation planning. Environ. Res. Lett. 16, 055022. https://doi.org/10.1088/1748-9326/abe74b

Gorelick, N., Hancher, M., Dixon, M., Ilyushchenko, S., Thau, D., Moore, R., 2017. Google Earth Engine: Planetary-scale geospatial analysis for everyone. Remote Sens. Environ., Big Remotely Sensed Data: tools, applications and experiences 202, 18–27. https://doi.org/10.1016/j.rse.2017.06.031

Gray, M.E., Zachmann, L.J., Dickson, B.G., 2018. A weekly, continually updated dataset of the probability of large wildfires across western US forests and woodlands. Earth Syst. Sci. Data 10, 1715–1727. https://doi.org/10.5194/essd-10-1715-2018

Hall, R.J., Skakun, R.S., Metsaranta, J.M., Landry, R., Fraser, R.H., Raymond, D., Gartrell, M., Decker, V., Little, J., Hall, R.J., Skakun, R.S., Metsaranta, J.M., Landry, R., Fraser, R.H., Raymond, D., Gartrell, M., Decker, V., Little, J., 2020. Generating annual estimates of forest fire disturbance in Canada: the National Burned Area Composite. Int. J. Wildland Fire 29, 878–891. https://doi.org/10.1071/WF19201

Harris, A., 2008. Spectral reflectance and photosynthetic properties of Sphagnum mosses exposed to progressive drought. Ecohydrology 1, 35–42. https://doi.org/10.1002/eco.5

Harvey, A.C., 1990. Forecasting, Structural Time Series Models and the Kalman Filter. Cambridge University Press, Cambridge. https://doi.org/10.1017/CBO9781107049994

Hernandez-Leal, P.A., Arbelo, M., Gonzalez-Calvo, A., 2006. Fire risk assessment using satellite data. Adv. Space Res., Natural Hazards and Oceanographic Processes from Satellite Data 37, 741–746. https://doi.org/10.1016/j.asr.2004.12.053

Hu, Y., Fernandez-Anez, N., Smith, T.E.L., Rein, G., 2018. Review of emissions from smouldering peat fires and their contribution to regional haze episodes. Int. J. Wildland Fire 27, 293. https://doi.org/10.1071/WF17084

Hyndman, R.J., Athanasopoulos, G., 2018. Forecasting: principles and practice. OTexts.

Juutinen, S., Virtanen, T., Kondratyev, V., Laurila, T., Linkosalmi, M., Mikola, J., Nyman, J., Räsänen, A., Tuovinen, J.-P., Aurela, M., 2017. Spatial variation and seasonal dynamics of leaf-area index in the arctic tundra-implications for linking ground observations and satellite images. Environ. Res. Lett. 12, 095002. https://doi.org/10.1088/1748-9326/aa7f85

Kong, M., Leblon, B., Mathieu, R., Gross, C.-P., Buckley, J., Naidoo, L., Bourgeau-Chavez, L., 2014. Use of Radarsat-2 polarimetric SAR images for fuel moisture mapping in the Kruger National Park, South Africa, in: 2014 IEEE Geoscience and Remote Sensing Symposium. Presented at the 2014 IEEE Geoscience and Remote Sensing Symposium, pp. 5033–5036. https://doi.org/10.1109/IGARSS.2014.6947627

Kruskal, W.H., Wallis, W.A., 1952. Use of Ranks in One-Criterion Variance Analysis. J. Am. Stat. Assoc. 47, 583–621. https://doi.org/10.1080/01621459.1952.10483441

Lastovicka, J., Svec, P., Paluba, D., Kobliuk, N., Svoboda, J., Hladky, R., Stych, P., 2020. Sentinel-2 Data in an Evaluation of the Impact of the Disturbances on Forest Vegetation. Remote Sens. 12, 1914. https://doi.org/10.3390/rs12121914

Leblon, B., Kasischke, E., Alexander, M., Doyle, M., Abbott, M., 2002. Fire Danger Monitoring Using ERS-1 SAR Images in the Case of Northern Boreal Forests. Nat. Hazards 27, 231–255. https://doi.org/10.1023/A:1020375721520

Lee, J.S., Jurkevich, L., Dewaele, P., Wambacq, P., Oosterlinck, A., 1994. Speckle filtering of synthetic aperture radar images: A review. Remote Sens. Rev. 8, 313–340. https://doi.org/10.1080/02757259409532206

Lees, K.J., 2021. Using remote sensing to assess peatland resilience by estimating soil surface moisture and drought recovery. Sci. Total Environ. 12.

Leuenberger, M., Parente, J., Tonini, M., Pereira, M.G., Kanevski, M., 2018. Wildfire susceptibility mapping: Deterministic vs. stochastic approaches. Environ. Model. Softw. 101, 194–203. https://doi.org/10.1016/j.envsoft.2017.12.019

Mann, H.B., 1945. Nonparametric Tests Against Trend. Econometrica 13, 245–259. https://doi.org/10.2307/1907187

Mansuy, N., Thiffault, E., Paré, D., Bernier, P., Guindon, L., Villemaire, P., Poirier, V., Beaudoin, A., 2014. Digital mapping of soil properties in Canadian managed forests at 250m of resolution using the k-nearest neighbor method. Geoderma 235–236, 59–73. https://doi.org/10.1016/j.geoderma.2014.06.032

Mariano, D.A., Santos, C.A.C. dos, Wardlow, B.D., Anderson, M.C., Schiltmeyer, A.V., Tadesse, T., Svoboda, M.D., 2018. Use of remote sensing indicators to assess effects of drought and human-induced land degradation on ecosystem health in Northeastern Brazil. Remote Sens. Environ. 213, 129–143. https://doi.org/10.1016/j.rse.2018.04.048

Mattia, F., Le Toan, T., Souyris, J.-C., De Carolis, C., Floury, N., Posa, F., Pasquariello, N.G., 1997. The effect of surface roughness on multifrequency polarimetric SAR data. IEEE Trans. Geosci. Remote Sens. 35, 954–966. https://doi.org/10.1109/36.602537

McPartland, M.Y., Kane, E.S., Falkowski, M.J., Kolka, R., Turetsky, M.R., Palik, B., Montgomery, R.A., 2019. The response of boreal peatland community composition and NDVI to hydrologic change, warming and elevated carbon dioxide. Glob. Change Biol. 25, 93–107. https://doi.org/10.1111/gcb.14465

Meingast, K.M., Falkowski, M.J., Kane, E.S., Potvin, L.R., Benscoter, B.W., Smith, A.M.S., Bourgeau-Chavez, L.L., Miller, M.E., 2014. Spectral detection of near-surface moisture content and water-table position in northern peatland ecosystems. Remote Sens. Environ. 152, 536–546. https://doi.org/10.1016/j.rse.2014.07.014

Mhawej, M., Faour, G., Abdallah, C., Adjizian-Gerard, J., 2016. Towards an establishment of a wildfire risk system in a Mediterranean country. Ecol. Inform. 32, 167–184. https://doi.org/10.1016/j.ecoinf.2016.02.003

Michael, Y., Helman, D., Glickman, O., Gabay, D., Brenner, S., Lensky, I.M., 2021a. Forecasting fire risk with machine learning and dynamic information derived from satellite vegetation index time-series. Sci. Total Environ. 764, 142844. https://doi.org/10.1016/j.scitotenv.2020.142844

Michael, Y., Helman, D., Glickman, O., Gabay, D., Brenner, S., Lensky, I.M., 2021b. Forecasting fire risk with machine learning and dynamic information derived from satellite vegetation index time-series. Sci. Total Environ. 764, 142844. https://doi.org/10.1016/j.scitotenv.2020.142844

Millard, K., Richardson, M., 2018. Quantifying the relative contributions of vegetation and soil moisture conditions to polarimetric C-Band SAR response in a temperate peatland. Remote Sens. Environ. 206, 123–138. https://doi.org/10.1016/j.rse.2017.12.011

Millard, K., Thompson, D.K., Parisien, M.-A., Richardson, M., 2018. Soil Moisture Monitoring in a Temperate Peatland Using Multi-Sensor Remote Sensing and Linear Mixed Effects. Remote Sens. 10, 903. https://doi.org/10.3390/rs10060903

Mirmazloumi, S.M., Moghimi, A., Ranjgar, B., Mohseni, F., Ghorbanian, A., Ahmadi, S.A., Amani, M., Brisco, B., 2021. Status and Trends of Wetland Studies in Canada Using Remote Sensing Technology with a Focus on Wetland Classification: A Bibliographic Analysis. Remote Sens. 13, 4025. https://doi.org/10.3390/rs13204025

Neta, T., Cheng, Q., Bello, R.L., Hu, B., 2011. Development of new spectral reflectance indices for the detection of lichens and mosses moisture content in the Hudson Bay Lowlands, Canada. Hydrol. Process. 25, 933–944. https://doi.org/10.1002/hyp.7878

Neta, T., Cheng, Q., Bello, R.L., Hu, B., 2010. Lichens and mosses moisture content assessment through high-spectral resolution remote sensing technology: a case study of the Hudson Bay Lowlands, Canada. Hydrol. Process. 24, 2617–2628. https://doi.org/10.1002/hyp.7669

Papacharalampous, G., Tyralis, H., Koutsoyiannis, D., 2018. Predictability of monthly temperature and precipitation using automatic time series forecasting methods. Acta Geophys. 66, 807–831. https://doi.org/10.1007/s11600-018-0120-7

Parisien, M.-A., Snetsinger, S., Greenberg, J.A., Nelson, C.R., Schoennagel, T., Dobrowski, S.Z., Moritz, M.A., Parisien, M.-A., Snetsinger, S., Greenberg, J.A., Nelson, C.R., Schoennagel, T., Dobrowski, S.Z., Moritz, M.A., 2012. Spatial variability in wildfire probability across the western United States. Int. J. Wildland Fire 21, 313–327. https://doi.org/10.1071/WF11044

Passive Control Networks [WWW Document], 2022. URL https://webapp.csrs-scrs.nrcan-rncan.gc.ca/geod/data-donnees/passive-passif.php (accessed 5.20.22).

Pearson, K., 1900. X. On the criterion that a given system of deviations from the probable in the case of a correlated

system of variables is such that it can be reasonably supposed to have arisen from random sampling. Lond. Edinb. Dublin Philos. Mag. J. Sci. 50, 157–175. https://doi.org/10.1080/14786440009463897
Price, D., Alfaro, R., Brown, K., Flannigan, M., Fleming, R.A., Hogg, E.H., Girardin, M., Lakusta, T., Johnston, M., McKenney, D., Pedlar, J.H., Stratton, T., Sturrock, R.N., Thompson, I.D., Trofymow, J.A., Venier, L., 2013. Anticipating the consequences of climate change for Canada's boreal forest ecosystems. Environ. Rev. 21, 322–365. https://doi.org/10.1139/er-2013-0042
R: Classical Seasonal Decomposition by Moving Averages, 2022.
Rao, K., Williams, A.P., Flefil, J.F., Konings, A.G., 2020. SAR-enhanced mapping of live fuel moisture content. Remote Sens. Environ. 245, 111797. https://doi.org/10.1016/j.rse.2020.111797
Saatchi, S., Halligan, K., Despain, D.G., Crabtree, R.L., 2007. Estimation of Forest Fuel Load From Radar Remote Sensing. IEEE Trans. Geosci. Remote Sens. 45, 1726–1740. https://doi.org/10.1109/TGRS.2006.887002
Sen, P.K., 1968. Estimates of the Regression Coefficient Based on Kendall's Tau. J. Am. Stat. Assoc. 63, 1379–1389. https://doi.org/10.1080/01621459.1968.10480934
Tanase, M., Panciera, R., Lowell, K., Aponte, C., 2014. Monitoring live fuel moisture in semi-arid environments using L-band radar data. Int. J. Wildland Fire in press. https://doi.org/10.1071/WF14149
Tanase, M.A., Kennedy, R., Aponte, C., 2015. Fire severity estimation from space: a comparison of active and passive sensors and their synergy for different forest types. Int. J. Wildland Fire 24, 1062. https://doi.org/10.1071/WF15059
Tarnocai, C., 2009. The Impact of Climate Change on Canadian Peatlands. Can. Water Resour. J. 34, 453–466. https://doi.org/10.4296/cwrj3404453
Thompson, D.K., Parisien, M.-A., Morin, J., Millard, K., Larsen, C.P.S., Simpson, B.N., 2017. Fuel accumulation in a high-frequency boreal wildfire regime: from wetland to upland. Can. J. For. Res. 47, 957–964. https://doi.org/10.1139/cjfr-2016-0475
Thompson, D.K., Simpson, B.N., Beaudoin, A., 2016. Using forest structure to predict the distribution of treed boreal peatlands in Canada. For. Ecol. Manag. 372, 19–27. https://doi.org/10.1016/j.foreco.2016.03.056
Thompson, D.K., Simpson, B.N., Whitman, E., Barber, Q.E., Parisien, M.-A., 2019. Peatland Hydrological Dynamics as A Driver of Landscape Connectivity and Fire Activity in the Boreal Plain of Canada. Forests 10, 534. https://doi.org/10.3390/f10070534
Tian, X., Mcrae, D.J., Boychuk, D., Jin, J., Gao, C., Shu, L., Wang, M., 2005. Comparisons and assessment of forest fire danger systems. For. Stud. China 7, 53–61. https://doi.org/10.1007/s11632-005-0058-0
Turetsky, M.R., Benscoter, B., Page, S., Rein, G., van der Werf, G.R., Watts, A., 2015. Global vulnerability of peatlands to fire and carbon loss. Nat. Geosci. 8, 11–14. https://doi.org/10.1038/ngeo2325
Ulaby, F., 1974. Radar measurement of soil moisture content. IEEE Trans. Antennas Propag. 22, 257–265. https://doi.org/10.1109/TAP.1974.1140761
Ulaby, F.T., Aslam, A., Dobson, M.C., 1982. Effects of Vegetation Cover on the Radar Sensitivity to Soil Moisture. IEEE Trans. Geosci. Remote Sens. GE-20, 476–481. https://doi.org/10.1109/TGRS.1982.350413
Valdez, M.C., Chang, K.-T., Chen, C.-F., Chiang, S.-H., Santos, J.L., 2017. Modelling the spatial variability of wildfire susceptibility in Honduras using remote sensing and geographical information systems. Geomat. Nat. Hazards Risk 8, 876–892. https://doi.org/10.1080/19475705.2016.1278404
Waddington, J.M., Morris, P.J., Kettridge, N., Granath, G., Thompson, D.K., Moore, P.A., 2015. Hydrological feedbacks in northern peatlands. Ecohydrology 8, 113–127. https://doi.org/10.1002/eco.1493
WaddingtonJ.M, ThompsonD.K, WottonM, QuintonW.L, FlanniganM.D, BenscoterB.W, BaisleyS.A, TuretskyM.R, 2011. Examining the utility of the Canadian Forest Fire Weather Index System in boreal peatlands. Can. J. For. Res. https://doi.org/10.1139/x11-162
Whitman, E., Parisien, M.-A., Thompson, D.K., Hall, R.J., Skakun, R.S., Flannigan, M.D., 2018. Variability and drivers of burn severity in the northwestern Canadian boreal forest. Ecosphere 9, e02128. https://doi.org/10.1002/ecs2.2128

Widodo, J., Izumi, Y., Takahashi, A., Kausarian, H., Kuze, H., Sumantyo, J.T.S., 2018. Detection of Dry-Flammable Peatland Area by Using Backscattering Coefficient Information of ALOS-2 Data L-Band Frequency, in: 2018 Progress in Electromagnetics Research Symposium (PIERS-Toyama). Presented at the 2018 Progress in Electromagnetics Research Symposium (PIERS-Toyama), pp. 916–920. https://doi.org/10.23919/PIERS.2018.8598099
Wieder, R.K., Vitt, D.H., 2006. Boreal peatland ecosystems, Ecological studies. Springer, Berlin.
Zhang, Y., Lim, S., Sharples, J.J., 2016. Modelling spatial patterns of wildfire occurrence in South-Eastern Australia. Geomat. Nat. Hazards Risk 7, 1800–1815. https://doi.org/10.1080/19475705.2016.1155501

Zheng, G., Moskal, L.M., 2009. Retrieving Leaf Area Index (LAI) Using Remote Sensing: Theories, Methods and Sensors. Sensors 9, 2719–2745. https://doi.org/10.3390/s90402719